Theor Chem Acc (1997) 97:41–46

Theoretical
Chemistry Accounts

A minimal distortion localization of occupied orbitals in supermolecule calculations of intermolecular interactions

G. Reza Ahmadi*, **I. Røeggen**

Institute of Mathematical and Physical Sciences, University of Tromsø, N-9037 Tromsø, Norway

Received: 15 December 1996 / Accepted: 15 March 1997

Abstract. A minimal distortion localization procedure is devised for defining subsystems in super-molecule calculations on weakly bonded complexes. When a set of orbitals for the isolated subsystem have been chosen, the localized supersystem orbitals are obtained by minimizing the sum of the least-square deviations from the isolated subsystem orbitals. Test calculations are presented for the beryllium complexes Be_2, Be_3 and Be_4, and the neon dimer.

Key words: Localization – Supermolecule calculations – Weakly bonded complexes – Extended geminal models

1 Introduction

There are two main classes of computational models used in the study of intermolecular interactions: symmetry adapted perturbation theories (SAPT) and supermolecule (SM) models. A recent review of the SAPT is given by Jeziorski et al. [1]. The main virtue of the SAPT models is the interpretative feature of the models. The interaction energy can be analysed in terms of polarization, induction, exchange and correlation contribution. The main weakness of this class of models is the lack of computational feasibility, in particular when third and higher-order terms are considered. The SM models, on the other hand, are based on ordinary quantum chemistry models such as many-body perturbation theory and coupled-cluster models. The SM approach can then profit from the computational efficiency of several highly optimized quantum chemistry codes. However, the disadvantage of these models is also well-known: the lack of interpretability of the interaction energy or the intermolecular potential.

The extended geminal models [2, 3] and extended group function models [4, 5] developed by Røeggen and coworkers are a non-conventional SM model which also offers an interpretative scheme. The present state of a research programme based on extended geminal models is given in a recent article by Røeggen and Wind [6]. Within this approach the intermolecular potential can be expressed in terms of distortion energies, i.e. the increase in subsystem energies owing to the presence of partner subsystems, and electrostatic, induction and correlation interaction terms for the distorted subsystems. The definition of subsystems is a key element for applying this interpretative scheme. The definition is based on a localization of the occupied supersystem orbitals. Currently, a localization scheme based on minimizing the Coulomb repulsion between the corresponding electron pairs is being adopted. However, this localization procedure is not entirely satisfactory. We would like to study changes in orbital densities owing to the presence of the partner subsystems. However, a localization principle based on minimizing the Coulomb repulsion might occasionally create drastic changes in the localized orbitals when there is only an infinitesimal change in the supersystem geometry. For example, Ahmadi et al. [7] demonstrated this effect in the complex $Ar \cdot Na^+$. In this case an umbrella-like structure for the localized valence orbitals of argon is inverted for a certain internuclear distance R between $R = 3.8$ a.u. and $R = 4.2$ a.u. This drastic change of localized orbital structure cannot easily be attributed to the partner subsystem. It is most likely an artefact resulting from the adopted localization procedure.

In this work we shall introduce a minimal distortion localization (MDL) procedure. The key element is to force the supersystem orbitals to be as similar as possible to the isolated subsystem orbitals. Hence, a change in the orbitals can then be interpreted as a genuine physical change, i.e. resulting from the partner subsystems.

2 The MDL procedure

The supersystem comprises a set of closed shell subsystems. Usually, for any supersystem calculation we start by considering the isolated subsystems. The geometry of the subsystems is identical to the geometry of the subsystem in the complex. As a result of a restricted

---

* *Present address*: Nesna College, N-8700 Nesna, Norway
Correspondence to: G.R. Ahmadi

Hartree-Fock (RHF) calculation we have a set of occupied orbitals for the isolated subsystem A:

$$\left\{\varphi_i^{A,\text{sub}};\ i = 1, \ldots, N_{\text{occ}}^A\right\} ,$$

where N_{occ}^A is the number of doubly occupied orbitals in subsystem A. The *form* of the orbitals $\{\varphi_i^{A,\text{sub}}\}$ is in a sense arbitrary. The orbitals might be the canonical orbitals, localized orbitals based on a conventional localization procedure, or localized orbitals subjected to some symmetry restriction. The doubly occupied orbitals for the supersystem are denoted

$$\{\varphi_i^{\text{super}};\ i = 1, \ldots, N_{\text{occ}}^{\text{super}}\} ,$$

where

$$N_{\text{occ}}^{\text{super}} = \sum_A N_{\text{occ}}^A . \tag{1}$$

A projection operator is associated with the orbital space defined by the occupied supersystem orbitals:

$$P_{\text{occ}}^{\text{super}} = \sum_{i=1}^{N_{\text{occ}}^{\text{super}}} |\varphi_i^{\text{super}}\rangle\langle\varphi_i^{\text{super}}| . \tag{2}$$

The best choice, in a least-square sense, of localized supersystem orbitals having the smallest possible deviation from the orbitals for the isolated subsystems is simply given by

$$\hat{\varphi}_i^{A,\text{super}} = P_{\text{occ}}^{\text{super}} \varphi_i^{A,\text{sub}}, \quad i = 1, \ldots, N_{\text{occ}}^A , \tag{3}$$

and for all subsystems A. By assuming there is no linear dependence in the set $\{\hat{\varphi}_i^{A,\text{super}}\}$, the sets $\{\hat{\varphi}_i^{A,\text{super}}\}$ and $\{\varphi_i^{\text{super}}\}$ define within a constant identical RHF functions. Since, the set $\{\hat{\varphi}_i^{A;\text{super}}\}$ usually consists of non-orthogonal functions, the key problem is then to orthonormalize the orbitals $\{\hat{\varphi}_i^{A;\text{super}}\}$ in such a way that the deviation from $\{\hat{\varphi}_i^{A;\text{super}}\}$ is as small as possible. One choice could be to determine the localized orbitals $\{\varphi_i^{\text{super,loc}}\}$ such that the functional

$$\mathscr{L} = \sum_{i=1}^{N_{\text{occ}}^{\text{super}}} \langle \hat{\varphi}_i - \varphi_i^{\text{super,loc}} | \hat{\varphi}_i - \varphi_i^{\text{super,loc}} \rangle \tag{4}$$

has a minimum. For notational reasons, in Eq. (4) we have used

$$\{\hat{\varphi}_i\} \equiv \left\{\hat{\varphi}_i^{A,\text{super}}\right\} . \tag{5}$$

This particular choice is, however, not entirely satisfactory. Core and valence orbitals are given equal weights in the functional $\mathscr{L}$. It is physically more attractive to have the smallest changes for the core orbitals and the largest changes for the valence orbitals when we compare them with the corresponding orbitals for the isolated subsystems. Hence, we partition the orbitals $\{\hat{\varphi}_i\}$ in a set of subgroups:

$$\Omega_\mu = \left\{\hat{\varphi}_i^\mu;\quad i = 1, \ldots, N_\mu\right\}, \qquad \mu = 1, 2, \ldots . \tag{6}$$

The number of subgroups and the number of orbitals in each group depend on the character of the complex. The partition might be based on the shell structure of the atoms comprising the supersystem. The ordering of the subgroups is such that the orbital energies associated with subgroup Ω_n, are lower than the orbital energies associated with subgroup Ω_{n+1}. Two examples will illustrate this type of partition. For Ar_2 we partition the orbitals in three subgroups: the 1*s*-orbitals, the L-shell orbitals, and the valence orbitals. For the complex ArNe we partition the orbitals in four subgroups: the 1*s*-orbital of argon, the 1*s*-orbital of neon, the L-shell orbitals of argon, and the valence orbitals of argon and neon.

The next steps in the MDL procedure are then as follows:

1. Orthonormalization of the orbitals in subgroup Ω_1.
2. If there is more than one orbital in Ω_1, determine the localized orbitals $\{\varphi_i^{1,\text{super,loc}}\}$ by minimizing the functional
$$\mathscr{L}_1 = \sum_{i=1}^{N} \langle \hat{\varphi}_i^1 - \varphi_i^{1,\text{super,loc}} | \hat{\varphi}_i^1 - \varphi_i^{1,\text{super,loc}} \rangle . \tag{7}$$
3. For subgroups no. $n (n > 1)$, construct a set or orbitals, $\tilde{\Omega}_n = \{\tilde{\varphi}_i^n\}$, which are orthogonal to the localized orbitals in the preceeding subgroups, i.e.
$$\tilde{\varphi}_i^n = \hat{\varphi}_i^n - \sum_{p=1}^{n-1} \sum_{j=1}^{N} \varphi_i^{p,\text{super,loc}} \langle \varphi_i^{p,\text{super,loc}} | \hat{\varphi}_i^n \rangle , \quad i = 1, \ldots, N_n . \tag{8}$$
4. Orthonormalize the orbitals in subgroup $\tilde{\Omega}_n$.
5. If there is more than one orbital in subgroup $\tilde{\Omega}_n$, determine the localized orbitals by minimizing the functional
$$\mathscr{L}_n = \sum_{i=1}^{N} \hat{\varphi}_i^n - \langle \varphi_i^{n,\text{super,loc}} | \hat{\varphi}_i^n - \varphi_i^{n,\text{super,loc}} \rangle . \tag{9}$$

The MDL procedure then ensures that the innermost orbitals have the smallest deviation from the corresponding isolated subsystem orbitals.

The minimization of the functionals $\{\mathscr{L}_\mu\}$ is performed by a restricted second-order procedure [8]. Let $\mathscr{L}$ denote these functionals:

$$\mathscr{L} = \sum_{i=1}^{n} \langle \hat{\varphi}_i - \varphi_i^{\text{super,loc}} | \hat{\varphi}_i - \varphi_i^{\text{super,loc}} \rangle . \tag{10}$$

For simplicity we have deleted the sub/superscript μ. The orthonormal orbitals of $\tilde{\Omega}$ are denoted $\{\chi_i;\ i = 1, \ldots, N\}$. We then have

$$\varphi_i^{\text{super,loc}} = \sum_{k=1}^{N} \chi_k U_{ki}, \qquad i = 1, \ldots, N . \tag{11}$$

We further write

$$\underline{\underline{U}} = \exp\{\underline{\underline{T}}\} , \tag{12}$$

where $\underline{\underline{T}}$ is a real skew-symmetric matrix; i.e.

$$\underline{\underline{T}}^+ = -\underline{\underline{T}} . \tag{13}$$

The variational parameters are the independent matrix elements T_{pq}, where $p > q$. In the following we give the expressions for the gradient and the Hessian, which are required in the second-order procedure.

The gradient:

$$
\begin{aligned}
g_{pq} &= \left(\frac{\partial L}{\partial T_{pq}}\right)_0 \\
&= \sum_{i=1}^{N}\left\{-2\left\langle \hat{\varphi}_i \middle| A\frac{\partial \varphi_i^{\text{super,loc}}}{\partial T_{pq}}\right\rangle + 2\left\langle \varphi_i^{\text{super,loc}} \middle| \frac{\partial \varphi_i^{\text{super,loc}}}{\partial T_{pq}}\right\rangle\right\}_0 \\
&= 2\left\{\langle \hat{\varphi}_p|\chi_q\rangle - \langle \hat{\varphi}_q|\chi_p\rangle\right\} \ . \qquad (14)
\end{aligned}
$$

The Hessian:

$$
\begin{aligned}
G_{pq,rs} &= \left(\frac{\partial L}{\partial T_{pq}\partial T_{rs}}\right)_0 \\
&= \sum_{i}\left\{-2\left\langle \hat{\varphi}_i \middle| \frac{\partial^2 \varphi_i^{\text{super,loc}}}{\partial T_{pq}\partial T_{rs}}\right\rangle + 2\left\langle \varphi_i^{\text{super,loc}} \middle| \frac{\partial^2 \varphi_i^{\text{super,loc}}}{\partial T_{pq}\partial T_{rs}}\right\rangle + 2\left\langle \frac{\partial \varphi_i^{\text{super,loc}}}{\partial T_{pq}} \middle| \frac{\partial \varphi_i^{\text{super,loc}}}{\partial T_{rs}}\right\rangle\right\}_0 \\
&= -\{\langle \hat{\varphi}_s|\chi_p\rangle + \langle \hat{\varphi}_p|\chi_s\rangle\}\delta_{qr} - \{\langle \hat{\varphi}_r|\chi_q\rangle + \langle \hat{\varphi}_q|\chi_r\rangle\}\delta_{sp} \\
&\quad + \{\langle \hat{\varphi}_r|\chi_p\rangle + \langle \hat{\varphi}_p|\chi_r\rangle\}\delta_{qs} \\
&\quad + \{\langle \hat{\varphi}_s|\chi_q\rangle + \langle \hat{\varphi}_q|\chi_s\rangle\}\delta_{rp} \ . \qquad (15)
\end{aligned}
$$

3 Localization measures

To characterize the localization of the orbitals we use two concepts: the charge centroid and the charge ellipsoid. The charge centroids are a set of vectors defined on the basis of the expression for the electronic part of the electric dipole moment:

$$
\left\langle \Phi^{\text{RHF}} \middle| -\sum_{i=1}^{2N}\mathbf{r}_i \Phi^{\text{RHF}}\right\rangle = -2\sum_{K=1}^{N}\langle \varphi^K|\mathbf{r}\varphi^K\rangle = -2\sum_{K=1}^{N}\mathbf{r}^K \ . \qquad (16)
$$

The vector $\mathbf{r}^K$ is the average position, or charge centroid, of the two electrons associated with the spatial orbital φ^K. Following Robb et al. [9] and Csizmadia [10] we define a measure of the extension of the geminal one-electron density by means of the second-order moments of the position operator, using the charge centroid as a local origin. The second-order moments (or variance matrix) associated with the geminal Λ_K^{RHF} are defined by the relations

$$
\mathbf{M}_{rs}^K = \langle \varphi^K|(x_r - x_r^K)(x_s - x_s^K)|\varphi^K\rangle, \qquad r,s \in \{1,2,3\} \ , \qquad (17)
$$

where x_r^K is the rth component of the charge-centroid vector $\mathbf{r}^K$ defined in Eq. (14). Diagonalization of the variance matrix yields the charge ellipsoid. The eigenvalues $\{a_1, a_2, a_3\}$ of the matrix $(\mathbf{M}_{rs}^K)$ correspond to the squares of the half-axes of the ellipsoid. The standard deviations in three orthogonal directions are therefore given by

$$
\Delta l_i = a_i^{1/2}, \qquad i \in \{1,2,3\} \ . \qquad (18)
$$

The quantities $\{\Delta l_i\}$ can then be used as a measure of the extension of the geminal one-electron density. Furthermore, we may also use the volume of the ellipsoid as a single number of the extension of the geminal one-electron density

$$
V = \frac{4}{3}\pi \Delta l_i \Delta l_2 \Delta l_3 \ . \qquad (19)
$$

4 Test cases

In this section we shall apply the advocated MDL procedure to small beryllium clusters and the neon dimer. The beryllium clusters may be considered as strongly bonded complexes, while the neon dimer is a weakly bonded complex.

4.1 Be_2, Be_3 and Be_4

The adopted basis set for the beryllium complex is an uncontracted $[20s, 6p, 4d, 2f]$ set of Gaussian type functions (GTFs) contracted to $[10s, 6p, 4d, 2f]$. The exponents of the uncontracted s-type functions comprise an even-tempered set [11]: $\eta_i = \alpha\beta^i$; $i = 1, \ldots, 2s$; $\alpha = 0.01605838$ and $\beta = 2.20140406$. The uncontracted $(20s)$ set is contracted to $[10s]$ by keeping the 9 most diffuse functions uncontracted, and using the expansion coefficients of the atomic $1s$-orbital as contraction coefficients. The polarization functions are uncontracted and they are defined with spherical harmonics. The exponents of the polarization functions are all drawn from the set of exponents of the s-type functions; i.e. they all have the form $\eta'_i = \alpha'\beta^i$. For the p-, d- and f-type functions we have respectively α' equal to 0.0353510, 0.0778218 and 0.1713171.

In this work we use the Beebe-Linderberg two-electron integral approximation [12, 13] with an integral threshold set equal to 10^{-8} a.u.

For the isolated beryllium atom we use canonical orbitals. The charge centroids then coincide with the nuclear position. In Fig. 1 we display an intersection

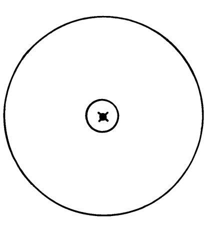

Fig. 1. Intersection between the *xy*-plane and the charge ellipsoids of the 1*s*- and 2*s*-orbitals of the beryllium atom. Charge centroids are marked with a *cross* and nuclear position with a *dot*

Table 1. Distances between charge centroids and the appropriate nucleus, half-axes and volumes of charge ellipsoids for beryllium complexes. The changes of the quantitites with respect to the values for the isolated atom, in parentheses[a]

	$\|\mathbf{r}^K - \mathbf{R}_1\|$ (a.u.)	Δl_1 (a.u.)	Δl_2 (a.u.)	Δl_3 (a.u.)	V (a.u.)
Be					
1*s*-orbital	0.0	0.278661	0.278661	0.278661	0.090639
2*s*-orbital	0.0	1.675895	1.675895	1.675895	19.716481
Be_2					
1*s*-orbital	0.000081	0.278718	0.278718	0.278726	0.090698
	(0.000081)	(0.000057)	(0.000057)	(0.000065)	(0.000059)
2*s*-orbital	0.211872	1.613118	1.613118	2.133576	23.255685
	(0.211872)	(−0.062777)	(−0.062777)	(0.457681)	3.539204
Be_3^{b}					
1*s*-orbital	0.000768	0.278711	0.278812	0.278856	0.090768
	(0.000768)	(0.000050)	(0.000151)	(0.000195)	(0.000129)
2*s*-orbital	0.792387	1.547911	1.824458	2.320770	27.453675
	(0.792387)	(−0.127984)	(0.148563)	(0.644875)	(7.737194)
Be_4^{c}					
1*s*-orbital	0.000833	0.278808	0.278808	0.278948	0.090829
	(0.000833)	(0.000097)	(0.000097)	(0.000092)	(0.000190)
2*s*-orbital	1.122522	1.751182	1.751182	2.362615	30.348997
	(1.122522)	(0.075287)	(0.075287)	(0.686720)	10.632516

[a] Interatomic distances are 4.32 a.u.

[b] Equilateral triangular structure

[c] Tetrahedral structure

between the *xy*-plane and the charge ellipsoids of the 1*s*- and 2*s*-orbitals. In this case of course, the ellipsoids are spheres. The lengths of the half-axes of ellipsoids are given in Table 1. The canonical 1*s*- and 2*s*-orbitals of the isolated beryllium atom are the reference orbitals which the MDL orbitals of the beryllium complexes should resemble as closely as possible.

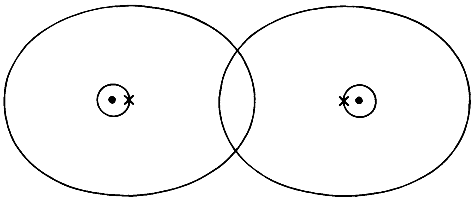

Fig. 2. Intersection between the *xy*-plane and the charge ellipsoids of the MDL orbitals of the beryllium dimer. The interatomic distance is equal to 4.32 a.u. Charge centroids are marked with a *cross* and nuclear positions with a *dot*

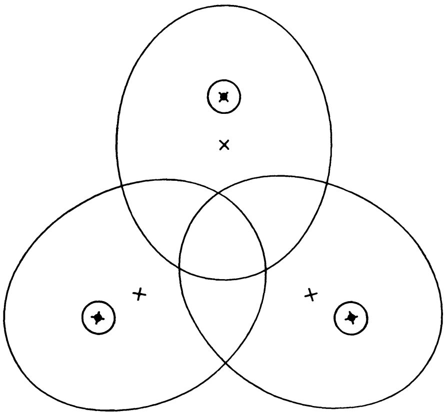

Fig. 3. Intersection between the *xy*-plane and the charge ellipsoids of the MDL orbitals of the beryllium trimer. The interatomic distance is equal to 4.32 a.u. Charge centroids are marked with a *cross* and nuclear positions with a *dot*

For beryllium complexes we consider the dimer, a trimer with equilateral triangular structure, and a tetramer with tetrahedral structure. All atomic distances are equal to 4.32 a.u., which is close to a bulk value for a h.c.p. structure [14]. When applying the MDL procedure, for all three complexes we partition the orbitals in two groups: the core orbitals and the valence orbitals. The results of the localization procedure are displayed in Table 1 and Figures 2–4. Pertaining to the results, we would like to emphasize the following points. First, as assured by the construction, the core orbitals are only slightly distorted. For the dimer, the charge centroids of the 1*s*-orbitals are shifted into the interatomic region. For the trimer and tetramer, the charge centroids of the core orbitals are shifted away from the interatomic region. The shifts increase with the number of atoms in the complex. Second, the distorted 2*s*-orbitals are shifted into the interatomic region. As for the core orbitals, the shifts increase with the number of atoms in the complex. The largest half-axis of the charge ellipsoid of a valence orbital is directed towards the centre of the geometrical structure of the complex. There is a large expansion of the orbital density along this axis, and increasing with the number of atoms in the complex. For the dimer the valence ellipsoids are contracted along the axes orthogonal to the interatomic axis. For the trimer, a valence ellipsoid has a small expansion along the second axis in the symmetry plane and a small contraction along the axis orthogonal to the symmetry plane. For the tetramer there are small expansions along both of the two shortest axes of a valence ellipsoid. We notice that the overlap between the charge ellipsoids of different valence orbitals increases when the number of atoms in the complex increases. A question that will be addressed in a forthcoming work is to what extent it is possible to have atom-like localization of the valence orbitals when the cluster Be_n approaches the bulk complex. The MDL approach should be an appropriate tool for analysing this problem.

4.2 The neon dimer

The basis set for the neon dimer is an uncontracted $[12s, 7p, 3d, 2f, 1g]$ set of GTFs contracted to $[6s, 4p, 3d, 2f, 1g]$. The s- and p-type functions are given by van Duijneveldt [15]. The $(12s, 7p)$ set is contracted to $[6s, 4p]$ by using the expansion coefficients of the atomic $1s$- and $2p$-orbitals as contraction coefficients, and keeping the five most diffuse s-type functions and the three most diffuse p-type functions uncontracted. The polarization functions are taken from the work of Dunning [16]. The set $[6s, 4p, 3d, 2f, 1g]$ is augmented with two additional sets of diffuse functions defined as an even-tempered extension of the subset in question. For the g-type functions we use the same quotient as for the f-type functions. Hence, the adopted basis set comprises a contracted $[8s, 6p, 5d, 4f, 3g]$ set of GTFs.

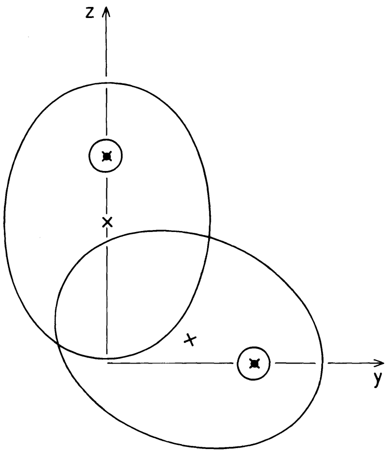

Fig. 4. Intersection between the xy-plane (a symmetry plane of Be_4) and the charge ellipsoids of two MDL orbitals of the beryllium tetramer. All interatomic distances are equal to 4.32 a.u. Charge centroids are marked with a *cross* and nuclear positions with a *dot*

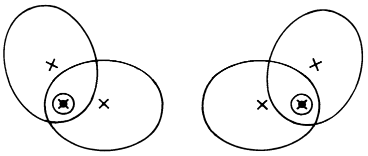

Fig. 5. Intersection between the xy-plane and the charge ellipsoids of MDL orbitals of the neon dimer. Interatomic distance is equal to 5.84 a.u. Charge centroids are marked with a *cross* and nuclear positions with a *dot*

The integral threshold used in the Cholesky decomposition of the two-electron matrix is set equal to 10^{-8} a.u.

The interatomic distance is 5.84 a.u., which is close to the assumed minimum of the interatomic potential [17].

The localized orbitals of the atomic neon are obtained by keeping the $1s$-orbital identical to the canonical $1s$-orbital and by performing a Boys localization [18] of the valence orbitals. Then we obtain four equivalent orbitals with a tetrahedral-like structure: i.e. the charge centroids of the valence orbitals coincide with the corners of a tetrahedron. For each of the isolated neon atoms we locate one valence charge centroid along the interatomic axis of the dimer. Hence, three charge centroids are pointing away from the neighbouring neon atom. Furthermore, the charge centroids outside the interatomic region are rotated to an eclipsed configuration (see Fig. 5). The MDL orbitals of the dimer should then resemble these localized atomic orbitals as closely as possible.

The results of the MDL procedure are given in Table 2. We notice that the $1s$-orbitals of the dimer are practically non-distorted. As for the two valence orbitals oriented along the interatomic axis, they are shifted slightly towards the nucleus of the atom they are part of. There is also a small contraction of all three axes of the charge ellipsoid of these two orbitals. As for the three equivalent orbitals of each atom, i.e. those pointing away from the neighbouring atom, the changes are an order of magnitude smaller than for the orbitals located in the interatomic region. We then expect that when we consider the electron correlation contribution to the interatomic potential for the neon dimer, the dominating contributions can be associated with the two orbitals located in the interatomic region. This is in fact the case. In another paper in this issue [19], an energy decomposition analysis of the interatomic potential demonstrates this feature.

Table 2. Distances between charge centroids and the appropriate nucleus, half-axes and volumes of charge ellipsoids for the neon atom and the neon dimer. The changes of the quantities with respect to the values for the isolated atom, in parentheses

	$\|\mathbf{r}^K - \mathbf{R}_1\|$ (a.u.)	Δl_1 (a.u.)	Δl_2 (a.u.)	Δl_3 (a.u.)	V (a.u.)
Ne					
$1s$-orbital	0.0	0.105623	0.105623	0.105623	0.004936
Valence orbital	0.451605	0.514760	0.514760	0.655456	0.727514
Ne_2^a					
$1s$-orbital	0.0	0.105623	0.105623	0.105623	0.004936
	(0.0)	(0.000000)	(0.000000)	(0.000000)	(0.000000)
t_1-orbital[b]	0.451393	0.514622	0.514622	0.655255	0.726901
	(−0.000212)	(−0.000138)	(−0.000138)	(−0.000201)	(−0.000613)
t_2-orbital[c]	0.451623	0.514762	0.514762	0.655438	0.727502
	(0.000018)	(0.000002)	(0.000002)	(−0.000018)	(−0.000012)

[a] Interatomic distance equal to 5.84 a.u.

[b] Orbital along interatomic axis, see Fig. 5

[c] One of three equivalent orbitals, pointing away from neighbouring atom, see Fig. 5

5 Concluding remarks

The MDL procedure solves the problem of defining subsystems in supermolecule calculations of intermolecular interactions. As demonstrated in the test calculations, it also allows for a detailed analysis of the changes of the orbital densities owing to complex formation. Even if the procedure is devised for a study of weakly bonded complexes, it might also be useful for a study of more strongly bonded systems. In particular, the MDL procedure is expected to be useful for a study of localization in large complexes of beryllium and magnesium.

Acknowledgements. All calculations reported in this work were performed on the CRAY J90 at NTNU, Trondheim, Norway. This work has received support from The Research Council of Norway through a grant of computing time.

References

1. Jeziorski B, Moszynski R, Szalewicz K (1994) Chem Rev 94:1887
2. Reggen I, (1983) J Chem Phys 79:5520
3. Røeggen I (1990) Int J Quantum Chem 37:585
4. Røeggen I, Ahmadi GR, Wind PA (1993) J Chem Phys 99:277
5. Røeggen I, Almlöf JE, Ahmadi GR, Wind PA (1995) J Chem Phys 102:7088
6. Røeggen I, Wind PA J Chem Phys (in press)
7. Ahmadi GR, Almlöf JE, Røeggen I (1995) Chem Phys 199:33
8. Roos B (ed) Springer Lecture Note series number 58
9. Robb MA, Haines WJ, Csizmadia IG (1973) J Am Chem Soc 95:42
10. Csizmadia IG (1975) In: Chalvet O, Daudel R, Diner S, Malrieu JP (eds) Localization and delocalization in quantum chemistry. Reidel, Dordrecht
11. Schmidt MW and Ruedenberg K (1979) J Chem Phys 71:3951
12. Beebe NHF and Linderberg J (1977) Int J Quantum Chem 12:683
13. Røeggen I and Wisløff-Nilssen E (1986) Chem Phys Letters 132:154
14. Emsley J (1994) The elements. Clarendon Press, Oxford
15. van Duijneveldt FB (1971) IBM Research Report RJ945
16. Dunning TH, Jr. (1989) J Chem Phys 90:1007
17. Aziz RA and Slamam MJ (1989) Chem Phys 130:187
18. Boys SF (1960) Rev Mod Phys 32:296
19. Røeggen I, Johansen T, J Mol Struct (Theochem) (to be published)